Atmospheric circulation patterns associated with extreme cold winters in the UK

Burgess, M. and Klingaman, N. P. ORCID: https://orcid.org/0000-0002-2927-9303 (2015) Atmospheric circulation patterns associated with extreme cold winters in the UK. Weather, 70 (7). pp. 211-217. ISSN 1477-8696 doi: https://doi.org/10.1002/wea.2476 Available at https://centaur.reading.ac.uk/38619/

To link to this article DOI: http://dx.doi.org/10.1002/wea.2476

Publisher: Wiley

Weather RMetS Royal Meteorological Society

Atmospheric Circulation Patterns Associated with Extreme Cold Winters in the UK.

Madlen Burgess and Nicholas P. Klingaman

Journal:	*Weather*
Manuscript ID:	WEA-14-0017.R3
Wiley - Manuscript type:	Research Article
Date Submitted by the Author:	08-Dec-2014
Complete List of Authors:	Burgess, Madlen; Met Office, Forecasting Sevice and Delivery Klingaman, Nicholas; University of Reading, National Centre for Atmospheric Science and Department of Meteorology
Keywords:	UK Extreme Winters, Twentieth Century Reanalysis dataset , South Westerly Winds

Atmospheric Circulation Patterns Associated with Extreme Cold Winters in the UK.

Madlen Burgess and Nicholas P. Klingaman

Introduction

Extremely cold winters have been observed in the UK since records began, but the exceptional temperatures during the winters of 2009/10 and 2010/11 greatly increased interest in this topic. With a mean temperature of -0.7ºC, December 2010 was the second coldest December in the Central England Temperature record (CET; Parker *et al.*, 1992) which dates to 1659, rivalling only December 1890 (-0.8 ºC). Previous research into the causes of such cold events have found associations with the North Atlantic Oscillation (NAO), Arctic Oscillation (AO), the East Atlantic Pattern (EA), the El Niño-Southern Oscillation (ENSO), blocking events and solar activity as discussed below. Many of these studies have been limited to the past 60-70 years due to a lack of four-dimensional reconstructions of atmospheric conditions (i.e. reanalysis data). This study uses the recently available 20th Century Reanalysis (Compo *et al.*, 2011) to provide the first reliable estimates of the state of the atmosphere during some of the coldest winters of the past 140 years, most of which have fallen outside the scope of past studies.

Known causes of UK cold winters

The NAO is the dominant mode of Northern Hemisphere extra-tropical atmospheric variability, describing oscillations in atmospheric mass between middle and high latitudes. Variability in this large-scale atmospheric circulation directly influences the risk of European seasonal temperature extremes (Scaife *et al.*, 2008). The NAO has a significant influence on the UK winter climate as its strongest variability and thus its greatest impact on the circulation, occurs during winter (George *et al*, 2004). A negative NAO reduces the meridional pressure gradient across the North Atlantic, due to either high pressure anomalies over Iceland, low pressure anomalies over the Azores or both; this weakens the climatological westerlies across northern Europe, resulting in less moisture and heat transport to the UK. This typically provides colder and drier winters than the positive NAO, when stronger westerlies result in warmer, wetter conditions. The AO is highly correlated with the NAO (Deser, 2000) and thus also influences winter surface air temperature variability (Thompson and Wallace, 2001). A negative AO is associated with a weak stratospheric polar vortex which allows intrusions of colder air to reach Europe, Asia and North America (Wang and Chen, 2009).

The EA is the second leading climate mode in the North Atlantic (Barnston, 1986). The structure of the anomalous pressure patterns are very similar in the EA as in the NAO, except that the anomaly centres are displaced south-eastwards. By altering the location and strength of the Atlantic pressure centres, the EA influences the location of the warm, moist jet over Europe and thus UK temperatures (Moore and Renfrew, 2012).

While the ENSO-NAO teleconnection has been rigorously investigated, the ENSO state provides only marginal predictive skill for European winter climate. Ineson and Scaife (2009) found that during El Niño, a quasi-stationary wave formed by the anomalously deeper Aleutian low can propagate into the stratosphere. This increases the probability of sudden stratospheric warmings, which in turn cause downward-propagating pressure anomalies that at the surface result in a negative NAO/AO pattern. Brönnimann (2007) also found that El Niño (La Niña) favours the negative (positive) NAO. However, this is not a straightforward, consistent relationship due to the large inter-event variability in ENSO strength, position and teleconnections. Its influence on winter-mean conditions is particularly difficult to clarify due to the potential reversal of the ENSO-driven sea-level pressure anomalies in the North Atlantic between early and late winter (Moron and Gouirand, 2003).

Other patterns of pressure anomalies can lead to extremely cold winters in the UK, such as blocking anti-cyclones. These conditions enhance extreme cold winters further through reducing cloud cover, allowing strong nocturnal cooling.

Anomalous sea surface temperatures (SST) in the North Atlantic have been found to modify the intensity and phase of the NAO due to local changes in surface evaporation, precipitation and heating (Rodwell *et al.*, 1999). In fact, Maidens *et al.* (2013) found that the main mechanism responsible for the extremely cold winter of 2010 was anomalous ocean heat content and associated anomalous North Atlantic SST. Autumn Siberian snow cover (Cohen and Jones, 2011) and Arctic sea ice (Yang and Christensen, 2012) have been shown to lead wintertime NAO variability, offering the possibility for statistical prediction of European winter climate.

Decadal and multi-decadal variations in solar activity have been associated with extreme UK winters (Lockwood *et al.,* 2010) but this is not a factor that is considered in this investigation. Stratospheric variability can also influence the NAO and hence Northern Hemisphere winter climate; the Quasi-Biennial Oscillation is the main driver on interannual temporal scales (e.g., Ebdon, 1975), while stratospheric sudden warmings can drive strong negative NAO phases on scales of weeks to months (e.g., Baldwin and Dunkerton, 2001).

A variety of factors and their interactions therefore can influence the frequency and intensity of extreme UK cold winters. This paper attempts to ascertain any large-scale atmospheric circulation patterns that are consistently associated with such extremes. An improved understanding of the causes of extreme cold winters may lead to more accurate forecasts and mitigate the social and economic impacts.

Motivation

Most of the studies discussed above employed reanalysis data to provide global, four-dimensional descriptions of the atmosphere. "Traditional" reanalyses, such as the European Centre for Medium-range Weather Forecasting 40-year reanalysis (ERA-40), require systematic upper-air observations, limiting their range to the period since World War II. As we show, this period contains very few of the extremely cold winters of the past 140 years. Here, we extend the period beyond and increase the sample size of extreme winters above previous studies (e.g., Hirschi and Sinha, 2007; Moore and Renfrew, 2012) by employing the 20th Century Reanalysis (20CR) which extends to 1871. We explore atmospheric conditions during winters never previously examined with such a comprehensive atmospheric dataset. This allows us to validate the conclusions of past research based on shorter time periods, as well as to investigate any common atmospheric circulation patterns associated with extremely cold winters in the UK.

Data

Created jointly by the National Centers for Environmental Predication (NCEP) and the National Center for Atmospheric Research (NCAR), the 20CR (Compo *et al.*, 2011) assimilates only surface pressure observations from the International Surface Pressure

Databank. Boundary conditions are provided by observed monthly sea-surface temperatures (SST) and sea ice from the Hadley Centre HadISST dataset (Rayner et al., 2003). To account for uncertainty due to the lack of upper-air data and the relative scarcity of surface-pressure observations early in the reanalysis period, particularly in the Southern Hemisphere, the 20CR consists of 56 ensemble members by employing an Ensemble Kalman Filter data assimilation scheme (e.g., Evensen, 2003). Six-hourly output is available for 1871-2010 at a 2˚ spatial resolution. Because the 20CR dataset ended on 31 December 2010 at the time of our study, we analyse winters from 1871-72 through 2009-10 (139 winters). Except where otherwise noted, this research uses the ensemble-mean, monthly and seasonal-mean 20CR data. SSTs anomalies are computed using HadISST.

Method

The most extreme cold winters in the UK during the 20CR period were identified by computing the detrended monthly and seasonal CET anomalies for December, January and Feburary (DJF) against the long-term mean. The detrended anomalies were then ranked from the most negative. No winter had high ranking (within the top ten) negative anomalies in all three months. We selected the seven winters with the largest negative DJF-mean detrended anomalies (hereafter "extreme winters"; Table 1), which had a mean anomaly of -2.5°C. The next (eighth) coldest winter had an anomaly of only -1.9°C. All extreme winters had at least one month in DJF which ranked within the top ten monthly anomalies; the winters of 1878, 1894 and 1962 had two such months. (All winters are referred to by the year in December.) We also directly compare December 2010 and December 1890, as the question of the similarity in the atmospheric circulations between these two extremely cold Decembers motivated this study. Six of the seven extreme winters – all except 1962 – are outside the scope of "traditional" reanalyses such as ERA-40; they could not be examined without long-period reanalyses such as the 20CR.

To validate 20CR surface temperatures over the UK, a 20CR CET was calculated and compared to observations. Reproducing the triangular area of the observed CET would have used only two 20CR grid points, which is likely below the effective resolution of the numerical model that produced the 20CR (e.g., Frehlich and Sharman, 2008). Instead, we averaged the eight 20CR grid points representing all UK land. We demonstrate that the 20CR CET reproduces the observed winter-to-winter variability (see Figure 1 below).

For each extreme winter, anomalies in mean sea level pressure (MSLP), SST, winds at 850 hPa, 500 hPa and 250 hPa, vertical velocities at 500 hPa and 700 hPa and specific humidity at 700 hPa and 850 hPa were examined. To reduce the influence of long-term climate change, anomalies were computed from a running 30-year seasonal mean, with the exceptions of DJF 1878 and December 2010, for which the means of the 1871-1900 and 1981-2010 respectively, were used.

To examine the influence of south-westerly flow on extreme cold winters, a South Westerly Index (SWI) was created based on the 850 hPa wind speed and direction in a region upstream of the UK (50-55°N, 18-10°W):

$$\mathbf{SWI} = \sqrt{(u^2 + v^2)}\ \cos[(\Theta - \pi/4)] \qquad (1)$$

where u is the box-averaged zonal wind, v the box-averaged meridional wind and θ is the angle of the box-averaged wind (where 0 is due westerly). The SWI was computed from six-hourly winds for all 20CR ensemble members; the "ensemble-mean" SWI is the mean SWI from all 56 members, not the SWI of the ensemble-mean 20CR winds.

Results

The 20CR ensemble mean accurately reproduces the winter-to-winter variability in CET (Figure 1); the correlation of DJF means with the observations is 0.98. However, the 20CR contains a substantial warm bias of 1.8°C, shown by the displacement of the 20CR values from the diagonal dashed line in Figure 1. This is likely because the UK is only at most two gridpoints wide at the 2° 20CR resolution; winter land temperatures are likely biased warm because of the influence of the surrounding sea points. The warm bias is greater in colder winters, probably due to a stronger land-sea temperature contrast. The extreme winters from the observations are also some of the most extreme winters in the 20CR dataset (Figure 1); the original, non-detrended observed and 20CR ensemble-mean CET values for these winters are given in Table 1.

Mean Sea Level Pressure

Figure 2 shows MSLP anomalies for a sample of the extreme winters. All extreme winters except 1890 (discussed further below) show negative anomalies south and west of the UK, along with positive anomalies to the north, exemplified by 1878 (Figure 2a) 1916 (Figure 2c) and 1939 (Figure 2d). These conditions recall the negative NAO, as they suggest a weakened Icelandic low and Azores high. This would result in a more southerly trans-Atlantic jet and cold and dry conditions in the UK. This relationship between negative NAO and cold UK winters has been widely accepted (Hurrell *et al*., 2003). The similarity in the MSLP patterns supports the hypothesis that while many factors may cause extreme winters, the effect of those factors is almost always communicated through a negative NAO.

A contingency table for DJF means of the observed NAO and CET indices demonstrates this relationship further (Table 2). These were constructed by sorting each index from low to high, dividing the resulting array into six equal sections, then assigning each DJF to a CET and NAO division. In each cell (i,j), we show the number of winters observed ($O_{i,j}$), as well as the number that would be expected ($E_{i,j}$) if the CET and NAO were unrelated, given by

$$E_{i,j} = \frac{\sum_{m-1}^{c} O_{i,m} \sum_{n-1}^{r} O_{n,j}}{N}$$

where c is the number of columns (6), r is the number of rows (6) and N is the number of winters (139). The much larger $O_{i,j}$ values compared to $E_{i,j}$ in the upper-left (lower-right) corners demonstrate a strong association between extremely negative (positive) NAO and very cold (warm winters). We performed a χ^2 test on the table for statistical significance, where

$$\chi^2 = \sum_{i=1}^{r} \sum_{j=1}^{c} \frac{(O_{i,j} - E_{i,j})^2}{E_{i,j}}$$

For Table 2, $\chi^2 = 104.39$, which indicates that we can reject the null hypothesis that the NAO and CET are unrelated at 99.5% confidence. A similar table was computed using all 56 20CR ensemble members (not shown); it shows a similar pattern, but overestimates the proportion of the coldest winters associated with the most negative NAO values.

This analysis supports the idea that the extreme winters occur during an extremely negative phase of the NAO. However, this is not the case for all years, as the pressure anomalies do not project perfectly onto the NAO structure. The influence of the AO can be seen in 1939 (Figure 2d), 1962 and December 2010 (Figure 2f). In addition, a south east shift in the anomalous pressure centres, shown by 1878 (Figure 2a), suggest the influence of the EA.

Interestingly, the winter of 1890/91 (Figure 2b) does not show a dipole of pressure anomalies, only a large anomalously positive MSLP over the UK. This pattern is shown more intensely by the December 1890 MSLP anomalies (Figure 2e), which suggests neutral NAO conditions with a large blocking anticyclone over and northeast of the UK, bringing colder air from continental Europe, in marked contrast to the negative AO/NAO pattern in December 2010. Further meteorological parameters are analysed to understand these results.

S*ea Surface Temperatures*

Global and North Atlantic sea surface temperature (SST) anomalies for all extreme winters demonstrate no consistent pattern (not shown). In contrast to the case study of 2010 in Maidens (2013), most extreme winters show only weak SST anomalies that vary in sign and magnitude between one extreme winter and the next.

Notable features are moderate positive SST anomalies in the equatorial Pacific in 1939, suggesting El Niño conditions (Figure 3b). In contrast, large negative SST anomalies off the coast of South America are found in 1916 (Figure 3a) and December 2010 (not shown), representing a strong La Niña. Pozo-Vazquez (2001) found a general association between La Niña and a positive phase of the NAO. The MSLP anomalies for the La Nina events in 1916 and December 2010 do not support this, however, as these winters were clearly negative NAO phases (Figure 2). The remaining extreme winters show no strong SST anomalies in the ENSO region.

Winds

Anomalous winds at 850 hPa (Figure 4), 500 hPa and 250hPa (not shown) for all extreme winters show anomalous easterlies over the UK, indicating an absence of the climatological south-westerly winds across the UK. All winters except 1890 have wind fields that resemble a classic negative NAO, with a more southerly jet into continental Europe, exemplified by 1878 (Figure 4a), 1916 (Figure 4c) and 1939 (Figure 4d). In 1890 (Figure 4b), the anomalous easterlies are instead associated with a large anti-cyclone over the North Sea, with anomalous westerlies over Scandinavia and easterlies across the continent. Regardless of the cause, all extreme winters are associated with reduced southwesterlies, which in some cases are replaced by mean easterlies or northeasterlies.

Figure 5a shows statistically significant (at the 5% level) positive 21-year windowed correlations between the ensemble-mean 20CR SWI and 20CR CET for each month in DJF, indicating that strong south westerly winds are associated with warmer temperatures in the UK. We note that there are periods of relatively weaker circulation-temperature relationships, particularly for January in 1900-1910 and for December in 1945-1965. Explaining these weaker correlations is outside the scope of this short study, but is clearly worth further research. The 20CR NAO also shows significant 21-year windowed correlations with the SWI (Figure 5b), suggesting that stronger south-westerly winds are found during the positive NAO. This agrees with the observed enhanced meridional pressure gradient across the North Atlantic that creates a stronger south-westerly jet. The CET-NAO correlation is more stable over time than for CET-SWI. A contingency table further demonstrates the overall strong relationship between the 20CR ensemble-member SWI and the CET (Table 3). A χ^2 test on this table indicates we can reject the null hypothesis that the 20CR SWI and CET are unrelated at the 99.9% confidence level (χ^2=3386.9). A table for the 20CR ensemble-member SWI and NAO was also statistically significant at the 99.9% confidence level.

Vertical Velocity

Analysis of vertical velocity anomalies at 700hPa and 500hPa diagnostics of convective activity in the extra-tropics and tropics, respectively, was inconclusive. The only consistent pattern found was anomalous ascent over the Maritime Continent and West Pacific (not shown). It is not clear how this affects the circulation anomalies over the Atlantic; further investigation would be necessary to determine a physical mechanism.

Specific Humidity

Specific humidity anomalies found drier conditions surrounding the UK at 850hPa for all extreme winters (not shown). These can be linked to the absence of south westerly winds as well as the anomalous easterlies that bring dry continental air to the UK. Anomalously moist conditions were seen in the Mediterranean, which can be explained by the anomalously displaced southerly jet bringing moisture from the Atlantic.

Discussion and Conclusions

This project examined common large-scale atmospheric circulation patterns during the seven most extremely cold UK winters in 1871-2010 using the 20CR. Prior to the introduction of the 20CR, it was not possible to analyse most of these winters because "traditional" reanalysis datasets rely on upper-air data and so extend to only the mid-twentieth century.

No single large-scale Northern Hemisphere atmospheric circulation pattern was associated with all seven extreme winters. The weakening of the climatological south-westerly winds over the UK, and in some cases the appearance of mean easterlies or north-easterlies, was found to be the dominant factor, but the change in the wind patterns had several causes. In all winters except 1890, the circulation resembled a negative NAO with varying degrees of contribution from the EA pattern. In 1890 however, a strong blocking anti-cyclone over the UK produced a similar effect on the wind patterns. To begin to understand and predict such extreme winters it is important to analyse the predictability of the direction and strength of the winds immediately upstream of the UK, as well as the predictability of the MSLP patterns that drive those wind patterns.

The analysis of the extreme winters, along with the NAO/CET contingency table (Table 2), supports the idea that most cold winters occur during negative NAO phases (Scaife *et al,.* 2008). Not all extremely negative NAO conditions led to extremely cold winters, however; Table 2 also showed that some milder winters occurred during highly negative NAO phases. There are similar outliers in the SWI/CET contingency table (Table 3), in which mild winters were associated with a lack of southwesterly winds. Further investigation is needed to understand why the association between the SWI and the CET sometimes breaks down. Figure 5a demonstrates that there have been particular decades, such as the 1960s, in which the SWI and CET display weaker 21-year windowed correlations for an individual month. With 56 ensemble members, the 20CR potentially provides a large sample of winters for future studies to investigate why the SWI and the CET became somewhat decoupled. While the ensemble members are not entirely independent, there is considerable intra-ensemble variability in the SWI, particularly early in the dataset, but little variability in CET (not shown). These periods of weaker SWI-CET correlations are an interesting and significant result, but understanding why this occurs is beyond the scope of this study.

SSTs, vertical velocities and specific humidity anomalies demonstrated no conclusive relationship with extreme cold winters. This analysis found no strong evidence that ENSO events influenced any examined periods. This result is significant as the broad statistical relationship between ENSO and UK temperature variability found by Pozo-Vazquez *et al*. (2001) was not reproduced through this case-study analysis. However this signal may have been masked by the reversal of the ENSO teleconnection from early to late winter, as found by Moron and Gouirand (2003).

Although noted as the coldest Decembers on record, few similarities were found between the Decembers of 1890 and 2010. The latter was associated with an intense negative NAO during a La Niña. In contrast, December 1890 showed no significant NAO or ENSO signal; instead anti-cyclonic blocking and easterly winds were found. This demonstrates that, although the NAO has been seen to be the most common feature throughout the examined winters, the most extreme conditions can occur in any favourable pressure pattern, so long as there is an absence of south-westerly winds.

Further analysis is required to investigate the alternative possible pressure patterns such as the EA and the AO in more depth. This would lead to a better understanding of their influence on south-westerly jets. Similar to the NAO analysis undertaken here, an index for both circulations could be created to determine any relationship with extremely cold winters. However none of the NAO, EA or AO explained the MSLP anomalies found during the winter of 1890. Analysis of additional extreme cold winters is also required to ascertain the influence of blocking events.

In addition, identifying common features in atmospheric conditions of the autumns prior to the extreme cold winters could prove to be essential for the predictability of cold winters. It has been shown that autumn snow cover in Eurasia (Cohen and Jones, 2011) as well as Arctic Sea Ice extent (Yang and Christensen, 2012) influence the NAO/AO and could therefore be drivers of European winter variability. If a relationship were found between autumn and winter conditions, it could improve the development and evaluation of dynamical and statistical seasonal forecast systems.

It is possible that the atmospheric circulation anomalies shown were diluted by analysing the DJF mean rather than the monthly means for extremely cold months. The magnitude of the anomalies for December 1890 and 2010 were much greater than the DJF three-month averages. To better understand the factors that contribute to extreme events it would be beneficial to examine the atmospheric conditions during only the extreme months.

This study has provided the first analysis of the atmospheric circulation patterns associated with some of the most extremely cold winters in the UK in the past 140 years. In doing so, the 20CR has been shown to provide dependable, realistic representations of past atmospheric conditions over the North Atlantic region into the late 19th century. It is suggested that future studies of UK winter climate use the 20CR to provide the longest possible estimate of past atmospheric conditions.

Acknowledgements

Dr. Nicholas Klingaman was supported by the National Centre for Atmospheric Science-Climate, a Natural Environment Research Council collaborative centre. Support for the Twentieth Century Reanalysis Project dataset is provided by the U.S. Department of Energy, Office of Science Innovative and Novel Computational Impact on Theory and Experiment program, and Office of Biological and Environmental Research, and by the National Oceanic and Atmospheric Administration Climate Program Office. The authors express their thanks to Dr. Gil Compo for providing timely 20CR data for 2010.

References

Baldwin MP, Dunkerton TJ. 2001. Stratospheric harbingers of anomalous weather regimes. *Science*, **294**: 581-584.

Barnston AG, Livezey RE. 1986. Classification, Seasonality and Persistance of Low-Frequency Atmospheric Circulation Patterns. *Mon. Weather Rev.,* **115**: 1083-1126.

Brönnimann S, Xoplaki E, Casty C *et al.* 2007. ENSO influence on Europe during the last centuries. *Climate Dyn.,* **28**: 181–197.

Cohen J, Jones J. 2011. A new index for more accurate winter predictions. *Geophys. Res. Lett*., **38**: L21701.

Compo GP and Coauthors. 2011. The Twentieth Century Reanalysis Project. *Q.J.Roy. Meteor. Soc*., **137**: 1-28.

Deser D. 2000. On the Teleconnectivity of the "Arctic Oscillation". *Geophys. Res. Lett.*, **27**: 779-782.

Ebdon RA. 1975. The quasi-biennial oscillation and its association with tropospheric circulation patterns, *Met. Mag.*, **104**: 282–297.

Evensen G. 2003. The Ensemble Kalman Filter: theoretical formulation and practical implementation. *Ocean Dynam.*, **53**, 343-367.

Frehlich R, Sharman R. 2008. The use of structure functions and spectra from numerical model output to determine effective model resolution. *Monthly Weather Review*, **136**, 1537-1553.

George DG, Jarvinen M, Arvola L. 2004. The influence of the North Atlantic Oscillation on the winter characteristics of Windermere (UK) and Paajarvi (Finland). *Boreal Environ. Res.,* **9**: 389-399.

Hirschi J J-M, Sinha B. 2007. Negative NAO and cold Eurasian winters: How exceptional was the winter of 1962/1963?. *Weather*. **62**: 43-48.

Hurrell JW. 2003. An overview of the North Atlantic Oscillation. The North Atlantic Oscillation: Climatic Significance and Environmental Impact, *Geophys. Monogr.,* **134**: American Geophysical Union, Washington, DC, 7–12.

Ineson S, Scaife AA. 2009. The role of the stratosphere in the European climate response to El Niño. *Nature Geoscience,* **2**: 32 – 36.

Lockwood M, Harrison RG, Owens MJ *et al.* 2011. The solar influence on the probability of relatively cold UK winters in the future. *Environ. Res. Lett.,* **6**: 11pp.

Maidens A, Arribas A, Scaife AA *et al.* 2013. The Influence of Surface Forcings on Prediction of the North Atlantic Oscillation Regime of Winter 2010/11. *Mon. Wea. Rev*., **141:** 3801-3813.

Moore GWK, Renfrew IA. 2012. Cold European winters: interplay between the NAO and the East Atlantic mode. *Atmosph. Sci. Lett*., **13**: 1–8.

Moron V, Gouirand I. 2003. Seasonal modulation of the ENSO relationships with sea level pressure anomalies over the North Atlantic in October–March 1873–1996. *Int. J. Climatol*., **23**: 143–155.

Parker DE, Legg TP, Folland CK. 1992. A new daily Central England Temperature Series, 1772-1991.*Intern. J. Climate,* **12**: 317-342.

Pozo-Vazquez D, Esteban-Parra MJ, Rodrigo FS *et al.* 2001. The Association between ENSO and Winter Atmospheric Circulation and Temperature in the North Atlantic Region. *J. Climate*, **14**: 3408-3420.

Rayner NA, Parker DE, Horton EB *et al.* 2003. Global analyses of sea surface temperature, sea ice, and night marine air temperature since the late nineteenth century. *Geophys. Res. Lett.*, **108**: 4407.

Rodwell M.J, Rowell DP, Folland CK. 1999. Oceanic forcing of the wintertime North Atlantic Oscillation and European climate. *Nature,* **398:** 320-323.

Scaife AA, Folland CK, Alexander LV *et al*. 2008. European Climate Extremes and the North Atlantic Oscillation. *J. Climate*, **21**: 72–83.

Thompson DWJ, Wallace JM. 2001. Regional climate impacts of the Northern Hemisphere annular mode. *Science*, **293**: 85–89.

Wang L, Chen W. 2010. Downward Arctic Oscillation signal associated with moderate weak stratospheric polar vortex and the cold December 2009. *Geophys. Res. Lett.*, **37**: L09707.

Yang, S., Christensen, JH. 2012. Arctic sea ice reduction and European cold winters in CMIP5 climate change experiments. *Geophys. Res. Lett.*, **39**: L20707.

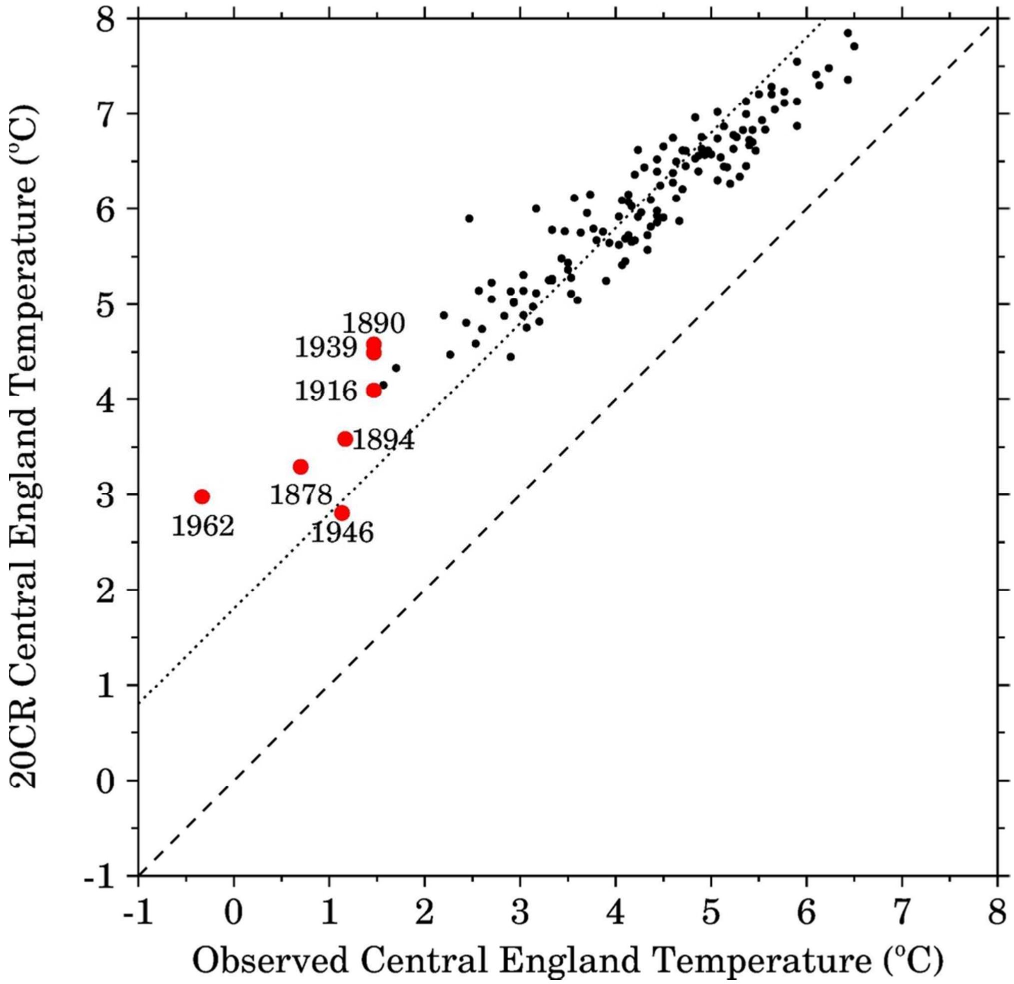

Figure 1: Scatter plot showing the ensemble mean 20CR CET (ºC) against the observed CET (ºC) for each winter between 1871-2009. Winters examined in this study are labelled and highlighted in red. The dashed line represents a perfect correspondence between observed and 20CR ensemble-mean CET, if the 20CR had zero mean bias. The dotted line represents a perfect correspondence, taking into account the 20CR ensemble-mean mean bias of +1.8C.
82x80mm (300 x 300 DPI)

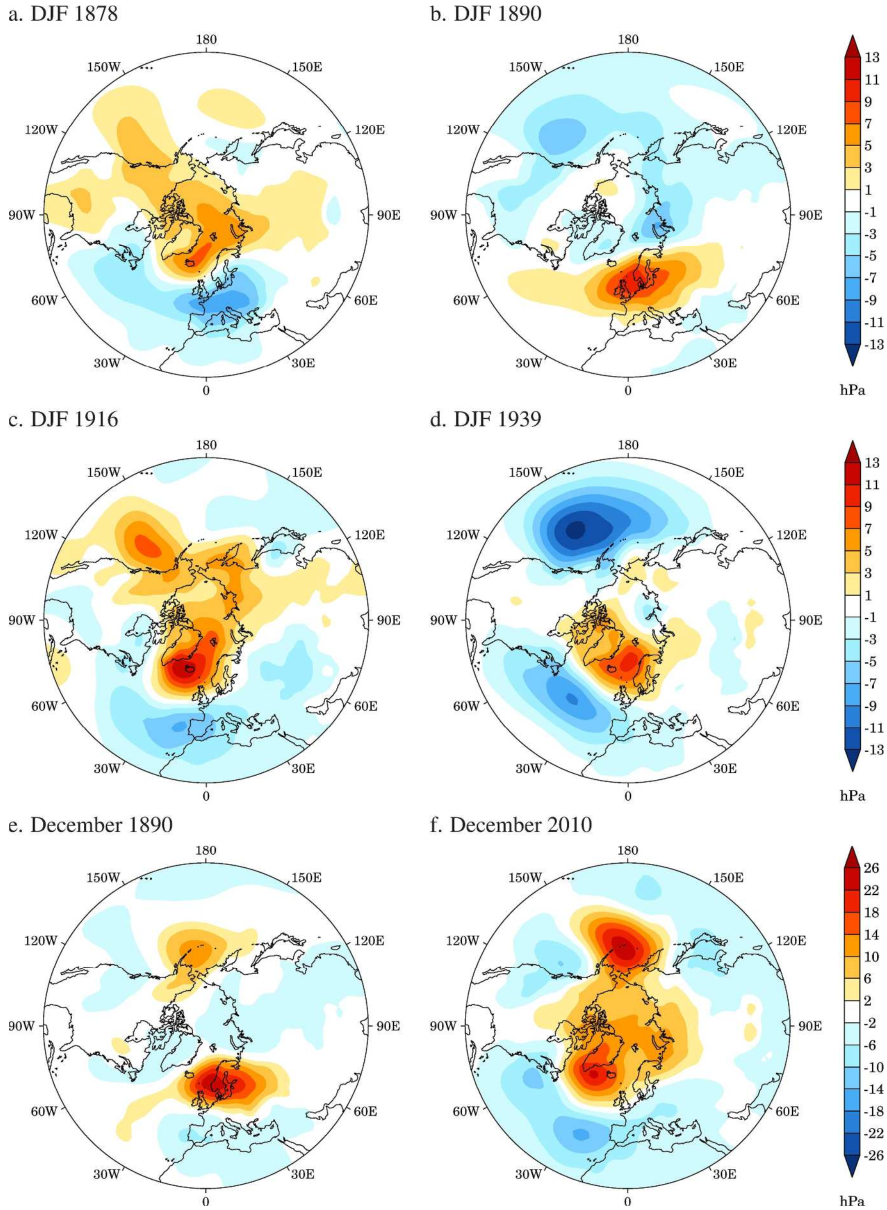

Figure 2: MSLP anomalies (hPa) for DJF a) 1878, b) 1890, c) 1916, d) 1939 and December e) 1890 and f) 2010. Anomalies are computed from the 30-year running mean, except for DJF 1878 and December 2010, for which we use the means of 1871-1900 and 1981-2010, respectively.
225x309mm (300 x 300 DPI)

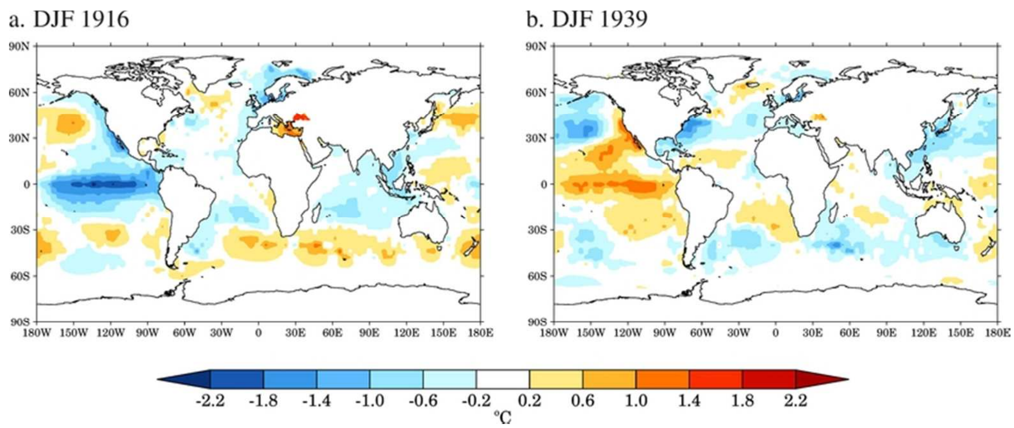

Figure 3: Sea Surface Temperature Anomalies (°C) with respect to the 30-year running mean for DJF a) 1916 and b) 1939.
71x29mm (300 x 300 DPI)

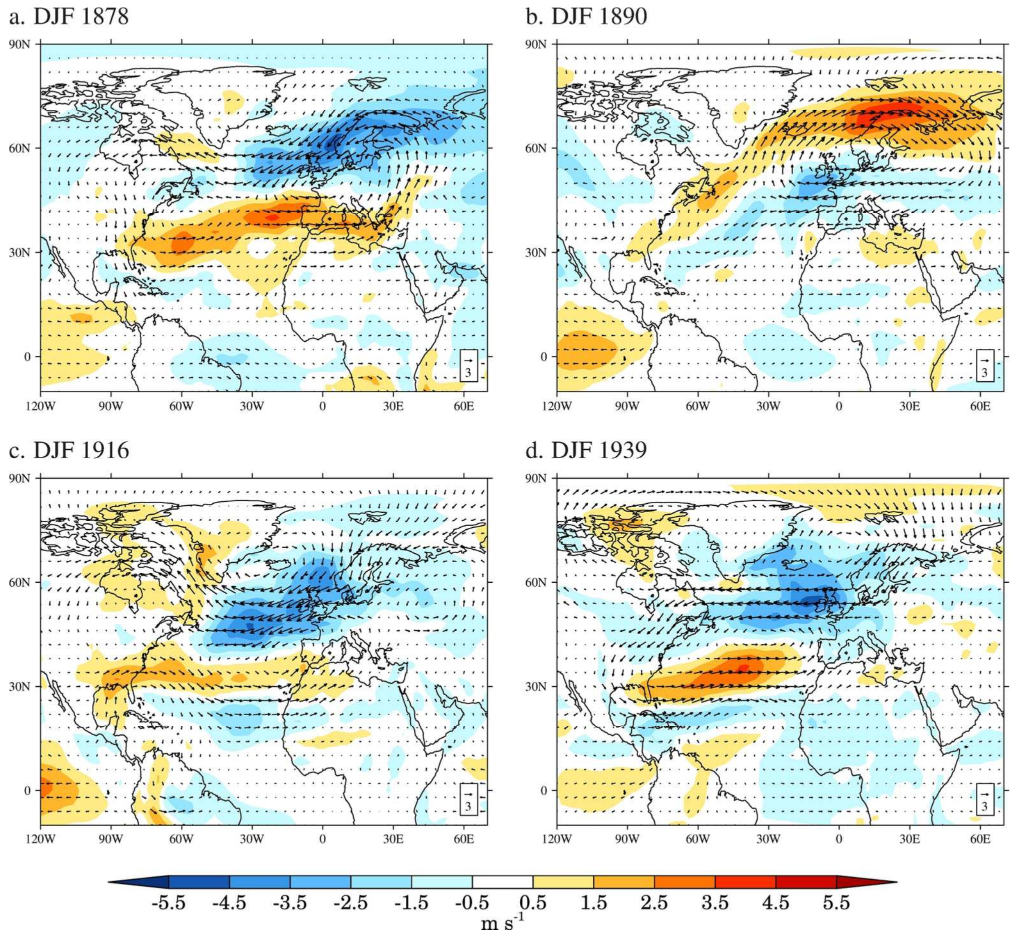

Figure 4: Vectors show anomalous 850 hPa winds (reference magnitude 3 m s-1) and shading shows anomalous 850 hPa wind speed (m s-1) during DJF a) 1878, b) 1890, c) 1916 and d) 1939. Anomalies were computed as for MSLP in Figure 2.
159x146mm (300 x 300 DPI)

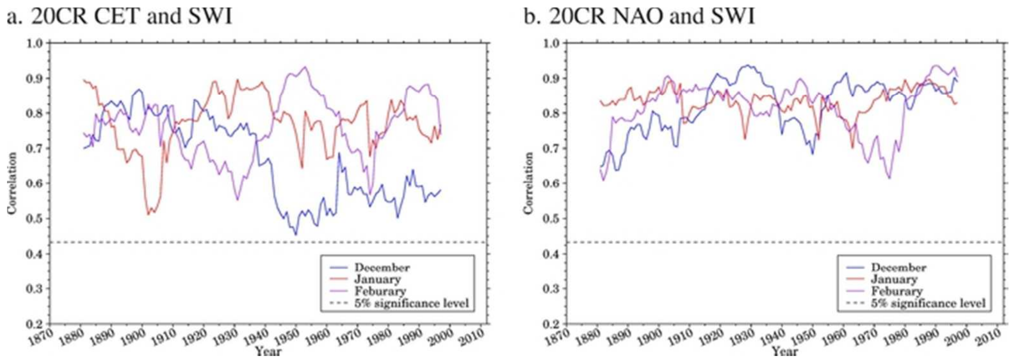

Figure 5: 21-year-windowed correlation between the monthly-mean, ensemble-mean 20CR SWI and a) 20CR CET and b) 20CR NAO for each winter month from 1871 to 2009. The dashed line indicates the 5% significance level. The year on the horizontal axis refers to the central year of the 21-year window.
60x21mm (300 x 300 DPI)

Table 1: Summary table showing the non-detrended, observed and 20CR values for CET and NAO as well as the ensemble-mean 20CR SWI for the identified extreme winters and for Decembers 1890 and 2010. The year for the winters refers to the year in December.

	Observed CET °C	20CR CET °C	NAO Index Observed hPa	NAO Index 20CR hPa	South Westerly Index ms^{-1}
Winter 1878	0.7	3.4	-1.61	-1.91	-0.12
Winter 1890	1.5	4.4	-0.43	-0.4	3.52
Winter 1894	1.2	3.7	-2.49	-2.58	-1.77
Winter 1916	1.5	4.2	-2.71	-2.57	-0.91
Winter 1939	1.5	4.5	-1.97	-1.90	1.48
Winter 1946	1.1	3.7	-1.55	-1.77	1.28
Winter 1962	-0.3	3.2	-2.77	-2.76	0.76
December 1890	-0.8	2.65	-3.05	-2.78	0.83
December 2010	-0.7	4.27	-4.92	-4.48	0.37

Table 2: A contingency table for observed DJF-mean NAO and CET for 1871-2009. The bold values on the top line of each cell show the number of winters for each joint division of NAO and CET values. The italicized values on the bottom line show the number of winters that would be expected if the NAO and CET were unrelated; these values are used for the χ^2 test reported in the text.

		NAO					
		Negative		Neutral			Positive
CET	**Cold**	**12** *3.81*	**8** *3.81*	**1** *3.81*	**1** *3.81*	**1** *3.81*	**0** *3.97*
	Cold	**9** *3.81*	**7** *3.81*	**3** *3.81*	**4** *3.81*	**0** *3.81*	**0** *3.97*
	Neutral	**1** *3.81*	**3** *3.81*	**7** *3.81*	**5** *3.81*	**5** *3.81*	**2** *3.97*
	Neutral	**0** *3.81*	**3** *3.81*	**7** *3.81*	**5** *3.81*	**6** *3.81*	**2** *3.97*
	Warm	**1** *3.81*	**2** *3.81*	**5** *3.81*	**3** *3.81*	**5** *3.81*	**7** *3.97*
	Warm	**0** *3.97*	**0** *3.97*	**0** *3.97*	**5** *3.97*	**6** *3.97*	**13** *4.18*

Table 3: As in Table 2, but for 20CR ensemble-member DJF-mean SWI and CET for 1871-2009.

CET	**SW Index**					
	Negative		Neutral			Positive
Cold	**546** *216.23*	**367** *216.23*	**211** *216.23*	**112** *216.23*	**56** *216.23*	**0** *206.83*
	421 *216.23*	**182** *216.23*	**267** *216.23*	**220** *216.23*	**198** *216.23*	**0** *206.83*
Neutral	**212** *216.23*	**317** *216.23*	**262** *216.23*	**243** *216.23*	**156** *216.23*	**98** *206.83*
	67 *216.23*	**249** *216.23*	**332** *216.23*	**216** *216.23*	**267** *216.23*	**157** *206.83*
Warm	**46** *216.23*	**173** *216.23*	**120** *216.23*	**168** *216.23*	**335** *216.23*	**446** *206.83*
	0 *206.83*	**0** *206.83*	**96** *206.83*	**329** *206.83*	**276** *206.83*	**531** *197.84*